Case Studies in Construction Materials 19 (2023) e02427

Contents lists available at ScienceDirect

Case Studies in Construction Materials

journal homepage: www.elsevier.com/locate/cscm

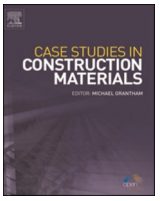

Case study

Laboratory-grade vs. industrial-grade NaOH as alkaline activator: The properties of coal fly ash based-alkaline activated material for construction

Teewara Suwan [a,*], Hong S. Wong [b], Mizi Fan [c], Peerapong Jitsangiam [a], Hemwadee Thongchua [d], Prinya Chindaprasirt [e]

[a] *Chiang Mai University Advanced Railway Civil and Foundation Engineering Center (CMU-RailCFC), Department of Civil Engineering, Faculty of Engineering, Chiang Mai University, Chiang Mai 50200, Thailand*
[b] *Department of Civil and Environmental Engineering, Faculty of Engineering, South Kensington Campus, Imperial College London, London SW7 2AZ, UK*
[c] *Department of Civil and Environmental Engineering, College of Engineering, Design and Physical Sciences, Brunel University, Uxbridge, London UB8 3PH, UK*
[d] *Department of Civil Engineering, Faculty of Engineering, Chiang Mai University, Chiang Mai 50200, Thailand*
[e] *Sustainable Infrastructure Research and Development Center, Department of Civil Engineering, Faculty of Engineering, Khon Kaen University, Khon Kaen 40002, Thailand*

ARTICLE INFO

Keywords:
Alkaline-activated material
Industrial-grade activator
Laboratory-grade activator
Production cost
Properties and microstructure

ABSTRACT

Alkaline-activated materials (AAM) are potentially low-carbon alternative binders for the cement industry. Most research studies related to AAM have been performed with high-purity laboratory-grade NaOH alkaline activators (Lab-grade). Gaining confidence in AAM beyond the laboratory scale in real applications remains a major challenge. To make this prospect more realistic, the viability of low-purity industrial-grade (Ind.-grade) and local no-grade alkaline activators was investigated. The strength results of Ind.-grade AAM were 15–20% lower than those of Lab-grade AAM. The purity of the Ind.-grade activator should be at least 98% to achieve the performance of Lab-grade AAM. The production cost of Ind.-grade AAM was 75–85% lower than that of Lab-grade AAM at the same activator concentration. It should be noted that the use of no-grade NaOH is not recommended for engineering purposes due to its uncertain quality and low purity. The combined benefits of low cost and high availability of Ind.-grade activators are expected to enhance the commercial viability of AAM as a sustainable alternative construction material for field applications.

1. Preamble

Ordinary Portland Cement (OPC) is the most widely used construction material that is critical for the built environment but emits a considerable amount of greenhouse gases (GHGs) because of the high-temperature processing and need for limestone calcination [1,2]. Over 4.1 billion metric tonnes of OPC are estimated to be manufactured globally annually [3]. The production of cement releases almost an equivalent amount of carbon dioxide (CO_2) into the atmosphere and this is a primary contributor to climate change. Many

* Corresponding author.
E-mail address: teewara.s@cmu.ac.th (T. Suwan).

https://doi.org/10.1016/j.cscm.2023.e02427
Received 6 June 2023; Received in revised form 8 August 2023; Accepted 24 August 2023
Available online 26 August 2023

attempts have been made to reduce, reuse, and recycle massive volumes of waste, in line with the United Nations Sustainable Development Goals (SDGs) [4,5]. Alternative cementitious binders have also been extensively studied to reduce the amount of OPC consumption. One approach to these alternative cementitious binders is alkaline-activated materials (AAM). Moreover, it has been shown that industrial by-products, e.g., coal combustion ash, have a high potential to be utilized as raw materials for the production of alternative binders.

AAMs have received increasing attention because they have the potential to partially reduce OPC consumption and simultaneously utilize a vast number of industrial wastes or by-products (e.g., fly ash, furnace slag, iron powder waste, and sludge ash) [6–9]. The production of AAM requires the use of strong alkaline solutions (e.g., NaOH and/or Na_2SiO_3) to activate the raw precursor materials to react and set. Heat curing (40–90 °C for 6–48 h) helps to accelerate the hardening process [10,11] and the properties of the hardened AAM have been reported as being similar to or better than those of OPC-based materials [12,13]. A huge body of research work has been carried out on AAMs. Major factors affecting the properties of AAMs are the: (i) raw precursor material, (ii) alkaline activator and dosage, (iii) type of AAM production, (iv) curing regime, and (v) manufacturing process [10,11,14,15].

However, most research studies related to AAM technology to date have been conducted on a laboratory scale where high-purity laboratory-grade alkaline activators are commonly used [13,16,17]. Although this ensures the performance, reliability, and consistency of the synthesized AAM, the cost of doing so is prohibitively expensive for routine field applications. Unfortunately, very few studies have been carried out using realistic industrial-grade alkaline activators and the effects of lower-grade activators on the properties of AAMs are not well understood. Therefore, this paper investigated the fresh and hardened state properties of fly ash-based AAM synthesized using several grades of activator. The overall aim is to uncover any performance differences attributable to the use of industrial-grade activators and to gain further confidence in the use of AAM beyond the laboratory scale. An evaluation of the material production cost per unit AAM was also undertaken. The authors envisage that the work will contribute to promoting the sustainable use of AAM in field applications by demonstrating its commercial viability as a coal combustion ash based-alternative construction material.

2. Activators for AAM

AAM is generally made from alumina-silicate minerals and alkaline activators, which dissolve the mineral components to initiate the process of reorganizing and polymerizing [18,19]. The alkaline activator is, therefore, a crucial factor that determines the final properties of the hardened AAM. Theoretically, alkaline metals and alkaline earth metals such as potassium/sodium hydroxide (KOH/NaOH), potassium/sodium silicate (K_2SiO_3/ Na_2SiO_3), sodium carbonate (Na_2CO_3), calcium hydroxide ($Ca(OH)_2$), or their combinations can be used in AAM synthesis [18–20]. However, sodium and potassium salts are more commonly used due to their strong alkaline properties, cost, and global availability [20–22]. Table 1 provides a brief review of the types and grades of alkaline activators, precursor material, curing conditions and the achieved compressive strength in several studies. The most widely used alkaline activators in AAM synthesis are NaOH, Na_2SiO_3, or their combination. It is also worth highlighting that coal combustion ashes (fly ash and bottom ash) are the main precursors used in coal based-power plant countries. Most previous studies were carried out using laboratory-grade activators on paste or mortar scale specimens. Of the studies reviewed, only one featured the use of an industrial-grade activator. Furthermore, it was found that the production cost of industrial-grade activators in large quantities is much lower than that of laboratory-grade activators.

The mechanical properties of AAM are generally improved by increasing the concentration of the alkaline activator [23] because it gives rise to a more substantial ion-pair formation and a faster and more complete poly-condensation of the precursor. The dissolution of alumina-silicate materials is also enhanced. However, an increase in the coagulated structure occurs at excessively high concentrations, leading to rapid formation and low workability. NaOH concentrations from 8 to 16 molars (M) and 30–50% w/w of Na_2SiO_3 are commonly used in AAM synthesis [10,31,32]. The activator-to-precursor material ratio, also known as the liquid-to-binder ratio (L/B), directly affects the workability of fresh AAM. Optimal L/B ratios from 0.26 to 0.45 have been suggested [10,17]. Apart from the type and concentration of the alkaline activator, consideration for grades, forms, ratios of the combined solution, and mixture

Table 1
Types and grades of alkaline activators for AAM synthesis.

No.	Alkaline activator		Alkaline activator grade	Sample Type	Comp. Strength		Starting Materials	Curing Condition		References
	Main (M)[a]	Addition			MPa	Age (d)		C°	hrs	
1	NaOH (12.5)	Na_2SiO_3	Lab-grade	Paste	95.0	28	FA class F[b]	85	20	[24]
2	KOH (7)	Na_2SiO_3	Lab-grade	Mortar	72.3	3	FA class F	85	24	[25]
3	NaOH (12)	-	Lab-grade	Mortar	70.4	28	FA class F	85	20	[26]
4	KOH (12)	K_2SiO_3	Lab-grade	Paste	70.0	28	FA and BA[c]	80	24	[23]
5	NaOH (-)	-	Lab-grade	Paste	67.0	28	GGBS[d]	38	90 d	[27]
6	Na_2SiO_3 (-)	-	Lab-grade	Paste	45.0	28	FA class F	60	28 d	[28]
7	NaOH (8)	Na_2SiO_3	Ind.-grade	Concrete	39.4	28	FA class F	80	24	[29]
8	NaOH (-)	Na_2CO_3	Lab-grade	Mortar	36.0	-	FA class F	85	20	[30]

[a] M = molarity
[b] FA class F = low calcium coal fly ash
[c] BA= coal bottom ash
[d] GGBS=ground granulated blast-furnace slag

proportions are also important.

NaOH is the focus of this study as it is commonly used in many industries, such as the manufacture of cleaning agents, paper, textiles, food and clothing. In 2016, it was reported that the annual production of NaOH was approximately 57–70 million tonnes globally, of which ~700k tonnes were in the UK and ~11 million tonnes in Europe [3,33]. It is manufactured in various grades and forms. In this work, the NaOH chemical analysis was carried out under the 'Thai Industrial Standard (TIS) 150: Sodium hydroxide for industrial uses', which conforms to 'ASTM E291: Standard test methods for chemical analysis of caustic soda and caustic potash (commercial grade)' and the 'BS 4130: Specification for sodium hydroxide (technical grades)'. No-grade NaOH was used to represent a local non-standard NaOH grade in this study.

Sodium hydroxide can be produced through different methods, mainly via the metathesis reaction between $Ca(OH)_2$ and Na_2CO_3, the LeBlanc process via Na_2CO_3 or electrolysis of NaCl [33–35]. The electrolysis of concentrated brine is the primary method for producing NaOH. Three types of electrolysis are used to produce NaOH of variable quality and purity [36], the membrane-cell process, the Nelson-diaphragm-cell process, and the mercury-cell process. A higher grade (or quality) of NaOH requires more energy and effort to produce, as presented in Fig. 1. Therefore, the reduced purity of industrial-grade activators has the potential to significantly reduce both raw material consumption and energy usage, consequently leading to a lesser environmental impact.

General-purpose NaOH flakes of 32%, 38%, 42%, 50%, and 62% purity are obtained from the first five processes, respectively. These low grades (sometimes called commercial/industrial grade) have lower selling prices than the high-standard laboratory grades. Less than 98% NaOH purity is generally found in local stores for household purposes as a No-grade NaOH. Therefore, the purity and composition of NaOH need to be verified for sensitive applications such as AAM synthesis. Table 2 shows the NaOH grades and components according to the Thai Industrial Standard (TIS) 150.

3. Materials

3.1. Coal ash

In this study, a high-calcium fly ash (FA-class C) obtained from the Mae Moh power plant in Lampang, Thailand was used. The specific gravity of the fly ash was measured to be 2.85. Its median particle size as determined with a dynamic light-scattering particle-size analyzer (Nanosizer-DLS) was 14.46 μm, while the specific surface area was 0.879 m^2/g. (Fig. 2). The chemical composition of the FA as determined with energy dispersive X-ray fluorescence (EDXRF, Malvern Panalytical) is shown in Table 3. In the present study, high-calcium fly ash Class C was utilized. For future investigations, a comprehensive exploration of different fly ash types and their respective properties will be conducted to further enhance our understanding of this area.

3.2. NaOH alkaline activators

Four NaOH activators, as shown in Fig. 3, were used in this study: laboratory-grade, industrial-grade class I, industrial-grade class II, and no-grade. Their particle morphology ranged from pearl-like to flaky particles of mm to cm scale in solid forms. The laboratory-grade NaOH was purchased from RCI Labscan Co., Ltd., Thailand, while the industrial-grades NaOH class I and II were supplied from Kusawad Chemical Group Co., Ltd., Thailand. The no-grade general/household purpose NaOH was purchased from a local store. This no-grade NaOH was used as a representative of non-standard grade NaOH, which can be found locally in Thailand. The bulk unit price of NaOH (per tonne) is shown in Table 4. Significant differences in the bulk unit price of NaOH materials were observed, with the

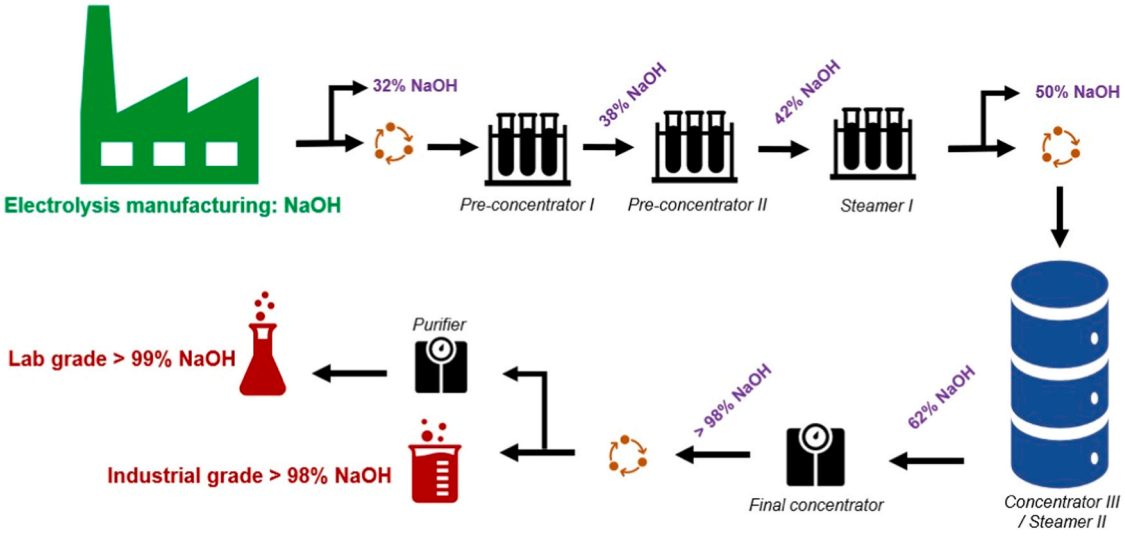

Fig. 1. Typical manufacturing processes for various purities/grades of NaOH [33–37].

Table 2
Composition of NaOH according to the Thai Industrial Standard (TIS) 150.

Component	Lab-grade	Specification (TIS 150)		No-grade
		Ind. Grade class I	Ind. Grade class II	
NaOH (% w/w)	> 99.0	> 99.0	> 98.0	< 98.0
Na_2CO_3 (% w/w)	< 1.0	< 0.5	< 2.0	(e.g., 32, 38, 42, 50, 62 etc.)
NaCl (% w/w)	< 0.0005	< 0.10	< 0.15	
Fe_2O_3 (% w/w)	< 0.0005	< 0.005	< 0.005	
$NaClO_3$ (mg./kg.)	-	< 100	< 200	

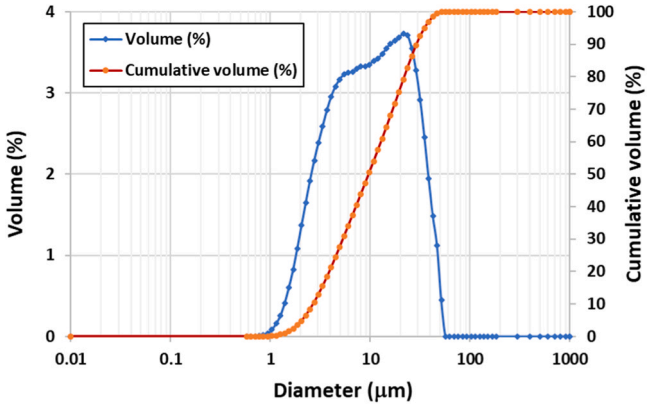

Fig. 2. Particle-size distribution of coal fly ash used in this study.

Table 3
Chemical composition (oxides) of coal fly ash by XRF analysis (%).

	SiO_2	Al_2O_3	SO_3	K_2O	CaO	TiO_2	MnO	Fe_2O_3	As_2O_3	SrO
Fly ash	20.05	9.38	5.34	2.59	30.96	0.68	0.25	30.34	0.08	0.30

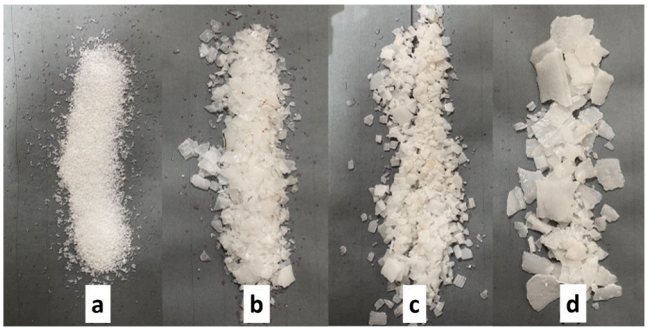

Fig. 3. NaOH samples of various grades: a) laboratory, b) industrial class I, c) industrial class II, and d) no-grade.

laboratory grade being at least 10 times more expensive than the no-grade. The NaOH was dissolved in deionized water to produce alkaline solutions with specific concentrations (in molar, M) for AAM.

4. Methodology

4.1. Mixture designation and sample preparation

Following an intensive review, NaOH concentration at 16 molars (16 M) was chosen in this study to compare the effect of NaOH grade on AAM properties. NaOH was weighed and dissolved in deionized water to produce a designated 16 M solution. It is noted that the final concentration of NaOH solution used in each mixture depends on the purity of the NaOH grade. The alkaline solutions were

Table 4
Bulk unit price of NaOH.

NaOH grade	Bulk unit price of NaOH per tonne (THB/£)*,* *
Laboratory grade	283,900 THB / £ 6740
Industrial grade class I	55,600 THB / £ 1320
Industrial grade class II	32,900 THB / £ 780
No-grade	26,900 THB / £ 640

*Pricing in Thai baht (THB) and pound (£) was based on the author's survey of Thailand's Northern region during 2021–2022.
* *£ 1 approx. 42.3 THB (Date: Nov 2022)

left for 24 h to ensure complete dissolution before use. Fly ash class C was weighed and placed in the 5-litre mortar mixer. Next, the prepared alkaline solution was added at a liquid-to-binder (fly ash) (L/B) ratio of 0.40. Wet mixing was carried out for 90 s at 140 ± 5 rpm at a room temperature of 28 ± 2 °C. After thorough mixing, the fresh AAM mixture was cast into 40 × 40 × 160 mm prism moulds (EN 196–1:2016) and wrapped immediately with plastic sheeting to prevent moisture loss. The samples were placed in the oven for curing at 60 °C for 24 h. Next, the samples were removed from the oven and allowed to cool down in an ambient environment. All samples were wrapped with plastic sheeting and kept at room temperature until reaching the required testing age.

4.2. Analytical techniques

Quantitative analysis of NaOH concentration (purity) was performed using an acid-base titration method, a common laboratory method for determining the concentration of an identified analyte with a standard solution of known concentration and volume. A digital pH meter (PH818 SmartSensor) was used to determine the pH values of the various prepared grades of NaOH solutions. The viscosity and rheology of each NaOH solution were determined using a digital viscometer (Brookfield DV–III Ultra Rheometer). It is noted that at least three sampling tests were done to define the average results.

A Vicat apparatus (ASTM C191) was used to determine the setting time of the fresh AAM paste, while a flow table (ASTM C230) was used to determine the flowability. Compressive and flexural strength tests were performed on a 250 kN universal testing machine (Control) on prism specimens with dimensions of 40 mm × 40 mm× 160 mm (BS EN 196–1). The samples were tested at the ages of 3, 28, and 60 days.

The composition and microstructure of the hardened AAM were analyzed via X-ray diffraction (XRD), Fourier Transform Infrared (FT-IR) analysis and scanning electron microscopy with energy-dispersive X-ray spectroscopy (SEM-EDS). XRD was carried out using a 4-circle kappa goniometer diffractometer with a microfocus sealed tube (Mo), direct photon-counting detector (HyPix-Bantam) and Cambridge Structural Database (CSD). FT-IR analysis was carried out using the attenuated total reflectance (ATR) technique on a Thermo Nicolet 6700 machine with spectral wavelength 450–4000 cm^{-1}. SEM-EDS was carried out using a JEOL JSM-5910LV equipped with lanthanum hexaboride cathodes, at 30 kV beam accelerating voltage and a minimum resolution of 2.0 nm.

5. Results and discussion

The results are outlined from the properties of various-grade NaOH solutions (the main focus of this study), the properties of fresh and hardened AAM mixtures, and their functional groups and microstructures.

5.1. Properties of alkaline activator (NaOH) solutions

The properties of various grades of NaOH solutions are shown in Table 5. All NaOH grades were prepared to 16-molar solution. By using the acid-base titration method, it was found that the average NaOH purity of the laboratory-grade sample (99.6%) was not significantly different from those of the two industrial-grade samples (99.5% and 98.7%). However, the purities of the no-grade NaOH sample was only 48.8%. In this study, the 48.8% purity NaOH was considered the best representative for 'no-grade' sodium hydroxide due to its widespread availability in local retail stores at a very affordable price. This suggests that the targeted NaOH concentration of 16 M (with >98% purity) may decrease significantly to around 8 M when using no-grade NaOH (<48.8%) in practical applications.

The concentration of activator plays a crucial role in AAM, as it governs the dissolution of alumina-silicate sources to produce reactive silica and alumina ion species. Consequently, a lower concentration may result in reduced degrees of dissolution and polymerization of AAM [17]. This, in turn, may potentially have a detrimental effect on the mechanical strength of the AAM, despite the

Table 5
Purity, pH value, and viscosity of various grades of NaOH solution.

NaOH grade	Standard	Avg. purity of NaOH (% / std. dev.)	pH	Avg. viscosity (cP)
Laboratory grade	TIS 150;	99.6% / (0.06)	12.38 ± 0.1	34.03
Industrial grade class I	ASTM E291;	99.5% / (0.05)	12.35 ± 0.1	33.67
Industrial grade class II	BS 4130	98.7% / (0.06)	12.27 ± 0.1	33.67
No-grade		48.8% / (0.75)	10.03 ± 0.1	27.50

favourable and cost-effective bulk unit price of no-grade NaOH. As a precautionary measure, it is essential to adopt a policy of rapid pre-testing of NaOH purity, utilizing methods such as portable titration units, before selecting NaOH for AAM production in real-case scenarios. For no-grade NaOH, it is noted that some small visible scattered dust particles were observed with high turbidity of the solution. These impurities are usually found in low-grade/price of NaOH flakes. Impurities in NaOH can arise from various sources (as shown in Table 2), including:

(i) Residual sodium chloride (NaCl) resulting from the electrolysis of brine.
(ii) Sodium carbonate (Na_2CO_3) formed during the carbonation and absorption of CO_2.
(iii) Sodium chlorate ($NaClO_3$) is generated as a side reaction during production.
(iv) Additional water (H_2O) due to the hygroscopic nature of atmospheric water.
(v) Metal ions introduced during manufacturing processes or storage.
(vi) Bulking agents used to increase the volume of the product.

However, laboratory-grade and industrial/commercial-grade NaOH typically undergo purification processes to minimize impurities and maintain consistent quality. Consequently, the purification of such grades of NaOH often results in purity levels exceeding 98%. Despite these efforts, it is common to find numerous industrial applications employing bulk materials to thicken the gross mass or serve as gelling agents, sizing agents, or adhesive additives [38,39]. One such commonly used bulk material is starch, a polysaccharide that is odorless, tasteless, and white in appearance, known for its ability to increase volume and stiffness. It can also serve as a backbone for partially biodegradable superabsorbent materials [40–42].

Within the scope of this study, it is confirmed that no-grade NaOH is unsuitable for engineering purposes due to the presence of impurities and the potential adverse effects on desired properties. This no-grade type of NaOH may find suitability for general household purposes. Nevertheless, further in-depth studies are planned to be undertaken in subsequent research work.

The Lab grade, Ind. grade I, and Ind. grade II achieved relatively high average pH values of 12.38, 12.35, and 12.27, respectively, while an average pH value of 10.03 was observed in the no-grade NaOH solution. Considering the concentration of OH ions in a 16 M NaOH solution, the expected pH range should be approximately 13–14. However, it has been observed that the measured pH can be lower than expected, which can be attributed to an alkaline effect. This effect occurs when H^+ ions in the gel layer of the pH-sensitive membrane are partially or fully replaced by alkali ions. Consequently, the measured pH appears lower than the actual number present in the sample. This phenomenon is commonly known as 'the alkali error' in pH testing [43]. As a result, pH values in the range of 10.03–12.38 may occur due to this alkali error. However, as expected, the higher NaOH purities resulted in alkaline solutions of higher pH values.

A Brookfield rheometer was used to examine the viscosity of NaOH solutions. The percentage of applied torque on the solution sampling was controlled from 85 to 100. The average viscosity of NaOH was reported in centipoise (cP). One cP equals one millipascal second (mPa s), referring to the attempt to rotate a standard tip in the sampling solution. The greater the cP value, the more viscous the liquid. For example, the viscosity at room temperature for freshwater = 1 cP, fresh milk = 3 cPs, honey = 10,000 cPs and ketchup = 50,000 cPs. Results show that the Lab and Ind. grades of NaOH had very similar average viscosity of around 33–34 cP, while the no-grade NaOH had a viscosity of only 27.5 cP. However, the alkaline activation could be decreased due to the reduced NaOH purity and pH.

5.2. *Fresh state properties of AAM*

Table 6 shows the initial setting time, flowability, and unit weight of AAM pastes produced with various NaOH grades. The initial setting times ranged between 70 and 210 min, which were well within the standard specification for Portland cement (ASTM C150) of not less than 45 min. It can be seen that the AAM-Lab mix achieved the quickest setting time. The industrial grade mixes took twice as long at around 2 h with little differences between AAM-Ind. I and II, while the AAM No-grade mix took over 3.5 h to set. The results suggest that reactivity decreases with a decrease in the purity of the NaOH activator used. The average flow values (122–132%) and the average unit weights (2.035–2.059 g/cm^3) showed no considerable difference between mixes. Due to the absence of a specified grade, it can be presumed that the no-grade NaOH used in the study contains a relatively low concentration due to the presence of bulking agents and impurities. As a result, a lower viscosity was observed, as depicted in Table 5. This characteristic renders the no-grade NaOH more favorable for AAM workability in comparison to higher-grade alternatives, as evidenced by its superior flow (132.4%) and lower unit weight (2.035 g/cm^3).

Table 6
Physical properties of AAM pastes produced in various NaOH grades.

Mixture	Setting time (min.)	Avg. Flowability (%)	Avg. Unit weight (g/cm^3)
AAM-Lab	70	122.5	2.043
AAM-Ind. I	122	123.2	2.059
AAM-Ind. II	147	121.9	2.041
AAM-No-grade	210	132.4	2.035

5.3. Mechanical properties of AAM

Fig. 4 shows the average flexural strength and compressive strength of the AAM paste samples at 3, 28, and 60 days of age. It should be noted that 36 samples were tested for flexural strength and 72 samples for compressive strength, with a standard deviation of less than 8% for both properties. The 28-day flexural strength ranged between the maximum of 16.9 MPa and the minimum of 5.2 MPa, while the 28-day compressive strength ranged between the maximum of 36.3 MPa and the minimum of 21.8 MPa, respectively. The strengths slightly increased with curing time. The small difference in strengths with curing time was because the microstructural developments were chiefly completed within the first 24 h of the heat-curing process. The results showed that all the AAMs' flexural strengths were around 23–46% of their compressive strengths.

It is interesting to note that the strength values of the Lab-grade AAM are slightly higher compared to those of the Ind.-grade AAM at equivalent age. Overall, the mechanical properties of the Ind.-grade AAM were around 15–20% lower than those of the Lab-grade AAM. This occurred even though these mixtures were synthesized with NaOH of over 98% purity. In contrast, the no-grade AAM with reduced purity NaOH of 48.8% achieved only ~22 MPa in compressive strength, which is nearly 40% lower than that of Ind.-grade AAM. This suggests that industrial-grade NaOH (Ind. I and Ind. II) has good potential for large-scale structural applications, while no-grade NaOH is probably only useful for low-strength applications.

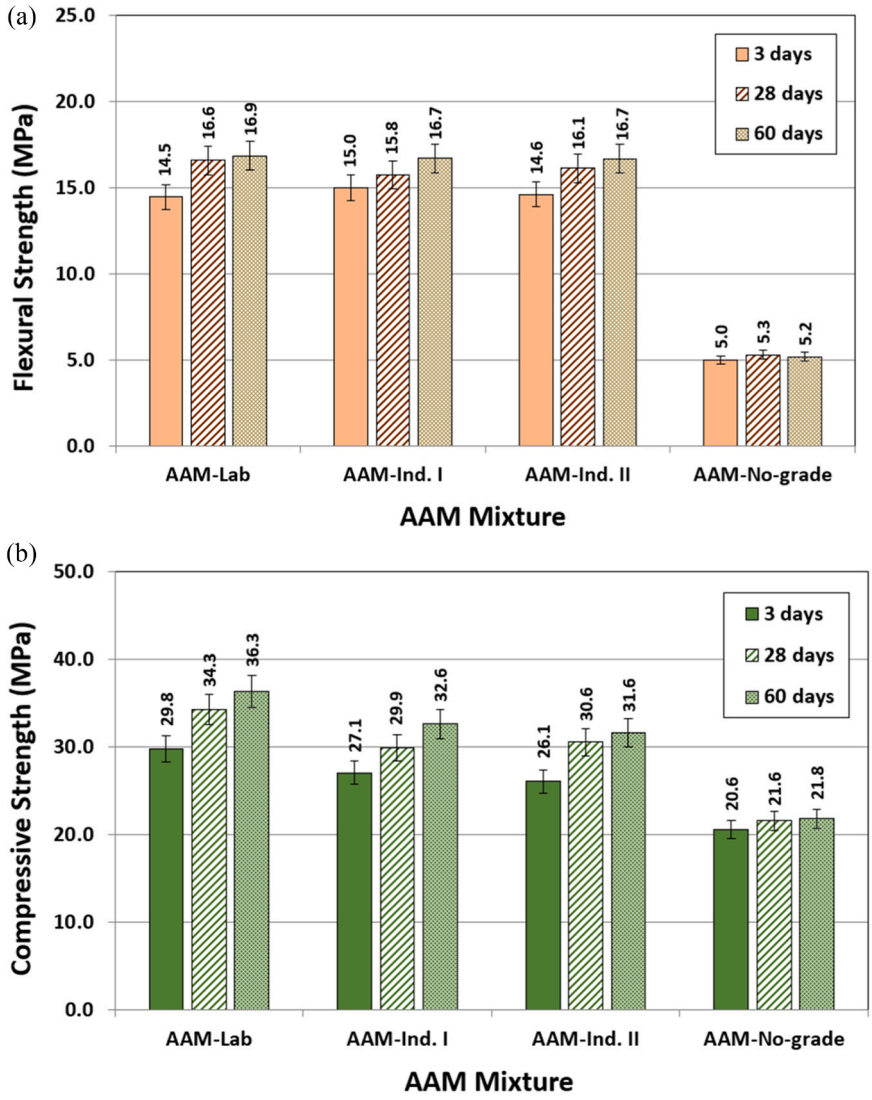

Fig. 4. Flexural strength and compressive strength of AAM mixtures.

5.4. Functional groups and structural composition

It is important to note that the particle shape, size and fineness of fly ash play a critical role in determining the mechanical properties of the AAM after activation. Smaller particles with a higher surface area promote enhanced physical and chemical reactions during polymerization, including accelerated dissolution rate, efficient ion transportation, and the formation of alumina-silicate species. These factors exert significant control over the initial setting time and strength development in the AAM [38]. The properties of AAM are influenced by various factors, with the precursor being a crucial determinant. The BS EN 450–1 or ASTM C618 sets out the requirements for utilizing fly ash as a supplementary cementitious material in concrete and cementitious systems [10,13]. Generally, there are two primary classes of fly ash: Class F (low-calcium) derived from burning anthracite or bituminous coal, and Class C (high-calcium), resulting from burning sub-bituminous or lignite coal. Both classes offer the potential to produce viable AAM [15, 17].

The functional groups and structural formation of the fly ash-based AAM mixtures in various NaOH grades were studied using FT-IR analysis and X-ray diffraction analysis, respectively. The infrared spectra of the AAM mixtures (Fig. 5) show absorption bands at 1650 cm^{-1}, corresponding to the O-H stretching and O-H bending of water (H_2O) left in the mixtures. Si-O and Al-O asymmetric stretching vibrations were defined at the band around 1095 cm^{-1}, indicating an amorphous phase or fly ash vitreous aluminosilicate material. A reaction between the fly ash and the alkaline activator was associated with the band at 945–960 cm^{-1}, indicating the Si-O stretching vibration of the SiO_4 and AlO_4 of the C-S-H, C(N)-A-S-H, or mixed gels. Furthermore, the formation of C(N)-A-S-H provided strength to the AAM after the hardening process. The spectra at 670 and 620 cm^{-1} exhibited the combined characteristics of Si-O-Al bending or C-H out-of-plane bending and C-O-H broad twisting, which are generally found in fly ash-based AAM with NaOH as the activator [17,44–46]. However, all of the FT-IR spectra of the various tested NaOH grades were mostly identical. Therefore, the NaOH grade exerted very small (or no) effects on the bonding of AAM functional groups [47].

The XRD spectra (Fig. 6) for all AAMs revealed the presence of similar phases, predominantly quartz (Q), calcite (C) and ettringite (E). A typical formation of portlandite (P), in high calcium content, was also observed as a solid microcrystalline phase at around 18.5 two-theta degrees. The structure phase of C-S-H (C′) was the semi-crystalline C-S-H gels in the alkali-activated systems rather than typical amorphous gels that can be often found in the water-activated systems. Aluminium oxide (Al_2O_3) and silicon dioxide (SiO_2) present in the silicoaluminous raw fly ash were found in the form of mullite (M) as $Al_{4.68}$ $Si_{1.32}O_{9.66}$ from the Cambridge Structural Database (CSD) and a recent study [48], at around 14 two-theta degrees. Other Na, Ca, Al, and Si compounds (S) were also detected, for example, N-A-S-H or C-A-S-H gels. Goethite (G), a form of low-temperature sediment of iron mineral as FeO(OH) or $FeAl_2O_4$, was found in small quantities as indicated by the peak around 31.1 two-theta degrees in the hardened AAM pastes.

The strong peaks in the XRD spectra indicate the presence of crystalline phases, however, the broad hump observed between 10 and 45 two-theta degrees suggests the formation of amorphous phases of the alkaline-activated material. This was in line with previous studies, which found that the strength of AAM is mainly achieved from the amorphous phases of Al^{3+}, forming AlO^{4-} tetrahedra [44, 49]. It should be noted that at higher curing temperatures, a higher degree of polymerization with a more robust polymeric chain and denser matrices were formed through the amorphous phases. However, as demonstrated by the FT-IR results, the XRD patterns of the various tested NaOH grades were very similar, indicating that the microstructures of well-designed Ind.-grade AAM were in the same

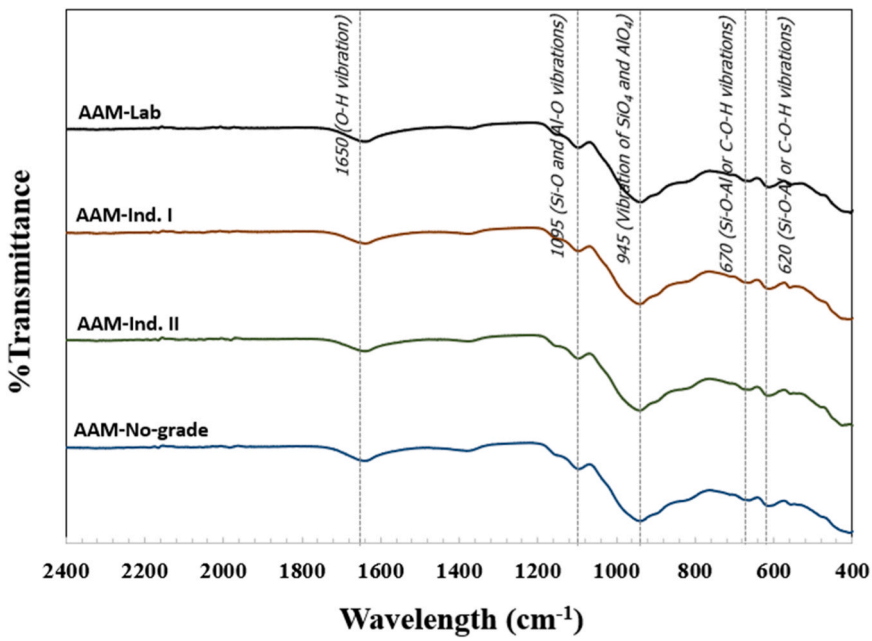

Fig. 5. FT-IR spectra of AAM with various NaOH grades at 28-day age.

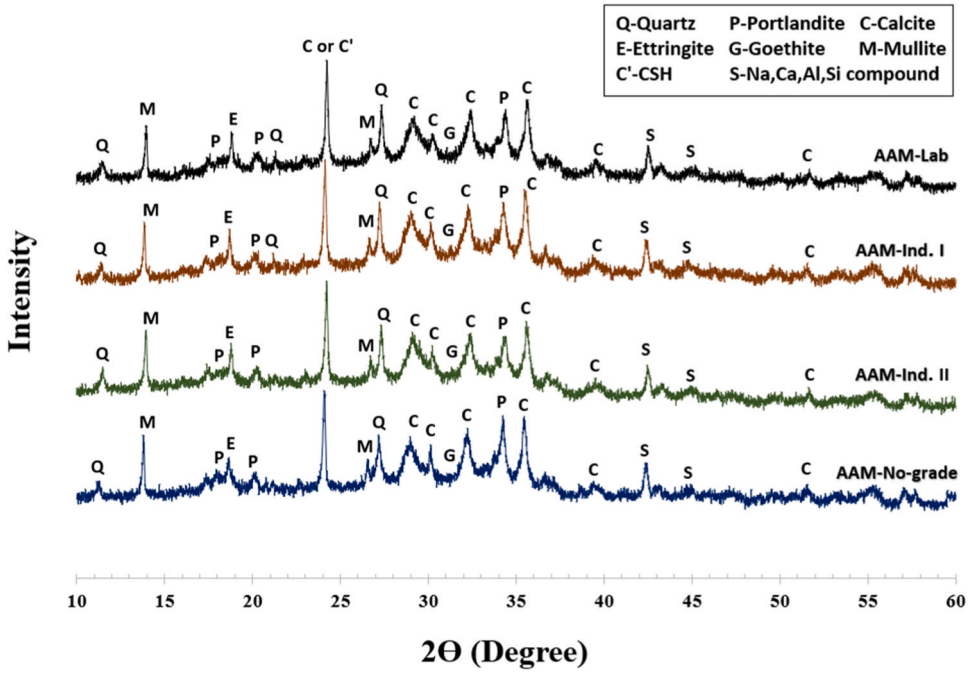

Fig. 6. XRD spectra of AAM with various NaOH grades at 28-day age.

order as those of typical Lab-grade AAM.

5.5. Microstructure

After the 28-day compressive strength test, selected broken pieces from each AAM mixture were collected and kept in a sealed plastic bag. All were immediately sent to SEM analysis within two hours on the same day of the crushing test. Selected SEM micrographs in the secondary electron mode of the AAM pastes are shown in Fig. 7a to d. The microstructure of all samples appears dense and compact due to the formation of amorphous AAM polymeric gel phases. Nevertheless, some unreacted fly ash particles were found and surrounded by scattered polymeric gel with visible microcavities in the Ind.-grade and No-grade AAMs.

SEM-EDS analyses were conducted on randomly selected points of the AAM-Lab mixture and the AAM-No-grade mixture for comparison. The results show that Si, Al, Ca, and Fe elements were detected as they are the main components of the raw starting material, fly ash. Sodium (Na) element was also detected due to the presence of the NaOH activator. The Si/Al and Ca/Si ratios in these mixtures were effectively within the range of those observed in previous studies [50]. Therefore, C-(A)-S-H gel (mainly Ca and Si contents) and (C,N)-A-S-H, or polymeric gel (indicated by substantial Si, Al, and Na contents), were formed.

5.6. Cost of AAM production and possible implications

The comparison of the production cost of AAM (per m^3) with various NaOH grades is presented in Table 7. It is noted that all references on cost are based on the authors' survey of bulk prices from Thailand market suppliers. The exchange rate of £ 1 was approximately 42.3 THB (November 2022). It only considers material costs with no inclusion of transportation or other production costs. The alkaline solution-to-fly ash ratio was set at 0.40 with 5% added water to maintain workability. The production cost of each primary material (November 2022) was OPC (£60.4/tonne), water (£3.5/tonne), fly ash (£11.6/tonne), sand (£10.5/tonne), and gravel (£12.8/tonne), respectively.

In general, the selling price of OPC strength class C25 (25 MPa) is around £ 42. However, AAM has a significantly higher production cost due to the cost of the alkaline activator (NaOH). The highest price was reached with the AAM-Lab mixture with 16 M-NaOH of ~ £ 394 per m^3, and this decreased to ~£ 156 per m^3 with 4 M-NaOH. The cost of AAM reduced substantially with industrial-grade or no-grade NaOH, to within the range of ~£ 38 to £ 98 per m^3, which becomes more comparable to OPC concrete of similar strength class.

Fig. 8a shows the production costs for all AAM concrete mixtures against NaOH grades. It can be seen that the AAM-Lab mixtures had the highest production cost for all NaOH concentrations, followed by AAM-Ind. I, AAM-Ind. II, and AAM-No-grade. The selected compressive strengths (Fig. 8b) of the AAM-Lab and AAM-Ind. II concrete mixtures with NaOH concentrations of 8 M and 16 M are also compared with the designed OPC concrete strength class of 25 MPa (£41.7/m^3). At 8 M-NaOH, the AAM-Ind. II (10.3 MPa) achieved slightly higher strength than the AAM-Lab (8.1 MPa), while its production cost was as little as around 1/5 of the typical AAM-Lab mixture (£52.5 and £254.5, respectively). At a high NaOH concentration of 16 M, the compressive strength of the AAM-Lab

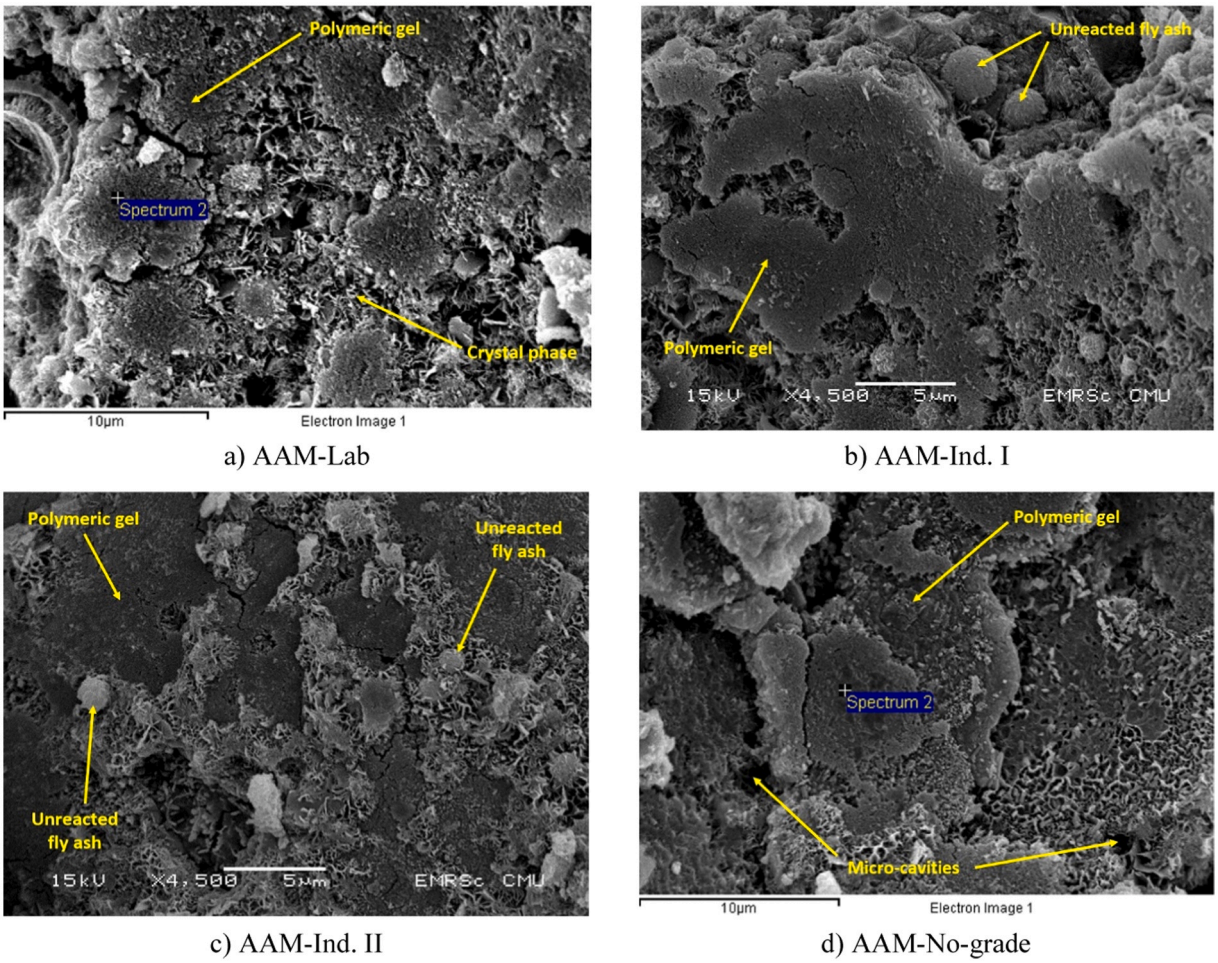

Fig. 7. SEM images of hardened AAM pastes with various NaOH grades.

achieved 34.3 MPa (£393.9/m^3), while the AAM Ind. II was 30.6 MPa (£68.5/m^3). Again, the compressive strengths of the 16 M-NaOH mixtures were not significantly different, but the Ind.-grade was almost six times cheaper [10,51].

Although the current production cost of AAMs is higher than that of normal OPC-based concretes, further research is expected to develop and improve the cost-effectiveness of AAMs for commercial markets in the near future. In the meantime, the achieved compressive strengths of the low-NaOH-concentration AAM-Industrial grades (e.g., 5 Molar) have surpassed the target compressive strength of cement-treated base (CTB) for pavements or unfired bricks of between 2.1 MPa and 7.0 MPa [51].

6. Conclusion

The fresh state properties, mechanical strengths and microstructure of high calcium fly ash-based AAM using conventional laboratory-grade (=99.6% NaOH), industrial-grade (>98% NaOH), and no-grade alkaline activators (<48.8% NaOH) cured up to 60 days have been investigated, including an evaluation of their production cost. The main conclusions are as follows:

1) The use of industrial-grade and no-grade NaOH activators increased the setting time (by a factor of 2–3), and increased flowability (by up to 10%) of fresh AAM due to the decrease in concentration, reactivity, and viscosity of the activator.
2) The flexural strength of AAM ranged between 5 and 17 MPa, while compressive strength ranged between 20 and 36 MPa for all mixtures. The measured strengths decreased with a decrease in the purity of the NaOH activator.
3) The mechanical properties of AAM produced using industrial-grade activators (>98% NaOH) were only 15–20% lower than those of typical laboratory-grade AAM. AAM produced using a no-grade activator (<48.8% NaOH) achieved the lowest strength. The results suggest that industrial-grade NaOH has good potential for large-scale structural applications, while no-grade NaOH is not recommended for engineering purposes due to its uncertain quality and low purity.

Table 7
The production cost of AAM concrete with various NaOH grades per cubic meter (m^3). *Note: Based on the Thailand market and suppliers.*

Mix	(M)	OPC		Water		Fly ash		Sand		Gravel		NaOH solid (£/tonne)	NaOH (solid form)								Unit weight (kg/m^3)	Unit cost (£/m^3)
													4 M		8 M		12 M		16 M			
		kg.	£	kg.	£	kg.	£	kg.	£	kg.	£		kg.	£	kg.	£	kg.	£	kg.	£		
OPC	-	323.0	19.5	170.0	0.59	-	-	825.0	8.63	1010.0	12.92	-	-	-	-	-	-	-	-	-	2328.0	41.68
AAM-Lab	4	-	-	128.0	0.45	350.0	4.07	825.0	8.63	1010.0	12.92	6740.0	19.3	130.1	-	-	-	-	-	-	2332.3	156.15
	8	-	-	113.0	0.39	350.0	4.07	825.0	8.63	1010.0	12.92		-	-	33.9	228.5	-	-	-	-	2331.9	254.50
	12	-	-	102.0	0.36	350.0	4.07	825.0	8.63	1010.0	12.92		-	-	-	-	45.4	306.0	-	-	2332.4	331.97
	16	-	-	92.0	0.32	350.0	4.07	825.0	8.63	1010.0	12.92		-	-	-	-	-	-	54.6	368.0	2331.6	393.95
AAM-Ind. I	4	-	-	128.0	0.45	350.0	4.07	825.0	8.63	1010.0	12.92	1320.0	19.3	25.5	-	-	-	-	-	-	2332.3	51.54
	8	-	-	113.0	0.39	350.0	4.07	825.0	8.63	1010.0	12.92		-	-	33.9	44.7	-	-	-	-	2331.9	70.76
	12	-	-	102.0	0.36	350.0	4.07	825.0	8.63	1010.0	12.92		-	-	-	-	45.4	59.9	-	-	2332.4	85.91
	16	-	-	92.0	0.32	350.0	4.07	825.0	8.63	1010.0	12.92		-	-	-	-	-	-	54.6	72.1	2331.6	98.02
AAM-Ind. II	4	-	-	128.0	0.45	350.0	4.07	825.0	8.63	1010.0	12.92	780.0	19.3	15.1	-	-	-	-	-	-	2332.3	41.12
	8	-	-	113.0	0.39	350.0	4.07	825.0	8.63	1010.0	12.92		-	-	33.9	26.4	-	-	-	-	2331.9	52.46
	12	-	-	102.0	0.36	350.0	4.07	825.0	8.63	1010.0	12.92		-	-	-	-	45.4	35.4	-	-	2332.4	61.39
	16	-	-	92.0	0.32	350.0	4.07	825.0	8.63	1010.0	12.92		-	-	-	-	-	-	54.6	42.6	2331.6	68.53
AAM-No-grade	4	-	-	128.0	0.45	350.0	4.07	825.0	8.63	1010.0	12.92	640.0	19.3	12.4	-	-	-	-	-	-	2332.3	38.42
	8	-	-	113.0	0.39	350.0	4.07	825.0	8.63	1010.0	12.92		-	-	33.9	21.7	-	-	-	-	2331.9	47.71
	12	-	-	102.0	0.36	350.0	4.07	825.0	8.63	1010.0	12.92		-	-	-	-	45.4	29.1	-	-	2332.4	55.03
	16	-	-	92.0	0.32	350.0	4.07	825.0	8.63	1010.0	12.92		-	-	-	-	-	-	54.6	34.9	2331.6	60.89

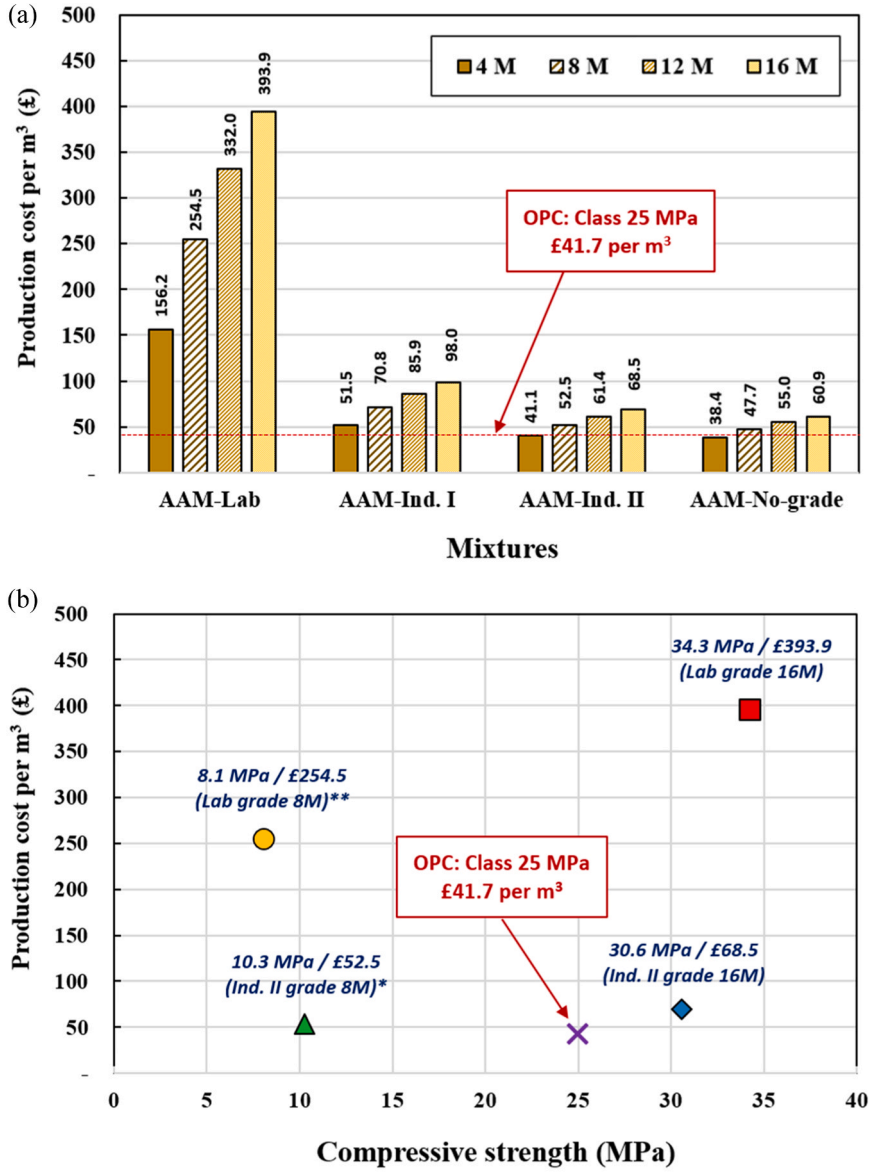

Fig. 8. Production cost and compressive strength of all AAM mixtures against various NaOH grades.

4) It is important to check the grade and purity of the activator to ensure acceptable performance of the resulting AAM. A rapid test (for example, by titration e.g., >98% NaOH purity for industrial-grade) may be used as a quality control/assurance measure to check the suitability of a particular activator for AMM production.
5) The production cost of AAM concrete ranged from £ 40 to £ 390 per m^3, which is significantly higher compared to conventional OPC concrete at a similar strength grade (C25, £41 per m^3). This is mainly due to the cost of the alkaline activator. Using an industrial-grade activator with a suitable (low) concentration could reduce the production cost of AAM to be comparable with OPC concrete of the same strength class.

Finally, the combined approach of using industrial-grade activators at a suitable concentration could increase the feasibility and commercial viability of AAM as an alternative construction material for field applications. With more knowledge from future research studies, the conversion of wastes into recycled-grade alkaline activators could also be used in the same manner as the presence of alkaline activators that could support the feasibility of AAM production onwards.

Declaration of Competing Interest

The authors declare that they have no known competing financial interests or personal relationships that could have appeared to

influence the work reported in this paper.

Data Availability

Data will be made available on request.

Acknowledgement

This work (grant no. RGNS 63–078) was supported by the Office of the Permanent Secretary, Ministry of Higher Education, Science, Research and Innovation (OPS MHESI), Thailand Science Research and Innovation (TSRI). Furthermore, this research work was partially supported by Chiang Mai University. The authors would like to express gratitude to the Department of Civil Engineering, Faculty of Engineering, Chiang Mai University (CMU), for providing equipment and facilities, as well as Mr. Witthawat Moonnee (M. Eng) who was working hard on this project. Special thanks to the cooperation of Brunel University London, UK and Imperial College London, UK. The last author would also like to acknowledge the support from the Research and Graduate Studies, Khon Kaen University.

References

[1] E. Allen, J. Iano, Fundamentals of building construction: Materials and methods, John Wiley & Sons, 2019 (Google book. Retrieved from), http://materialsmethods.pbworks.com/w/file/fetch/128566209/FBC%20Soil%20Retaining.pdf.
[2] K.K.G.K.D. Kariyawasam, C. Jayasinghe, Cement stabilized rammed earth as a sustainable construction material, Constr. Build. Mater. 105 (2016) 519–527.
[3] L. Fernández, 2022. Sodium hydroxide industry usage in Europe by end user 2020, statista. Retrieved from https://www.statista.com/statistics/931159/caustic-soda-applications-europe/ on May 7th, 2022.
[4] Lehne, J. and Preston, F., 2018. *Making concrete change: Innovation in low-carbon cement and concrete*.
[5] W. Ferdous, et al., Recycling of landfill wastes (tyres, plastics and glass) in construction–a review on global waste generation, performance, application and future opportunities, Resour., Conserv. Recycl. 173 (2021), 105745.
[6] M.H.N. Yio, et al., Effect of autogenous shrinkage on microcracking and mass transport properties of concrete containing supplementary cementitious materials, Cem. Concr. Res. 150 (2021), 106611.
[7] T. Bualuang, et al., Non-OPC binder based on a hybrid material concept for sustainable road base construction towards a low-carbon society, J. Mater. Res. Technol. 14 (2021) 374–391.
[8] T. Nongnuang, et al., Characteristics of waste iron powder as a fine filler in a high-calcium fly ash geopolymer, Materials 14 (10) (2021) 2515.
[9] H.S. Wong, et al., Hydrophobic concrete using waste paper sludge ash, Cem. Concr. Res. 70 (2015) 9–20.
[10] P. Jitsangiam, et al., Challenge of adopting relatively low strength and self-cured geopolymer for road construction application: a review and primary laboratory study, Int. J. Pavement Eng. (2019) 1–15, https://doi.org/10.1080/10298436.2019.1696967.
[11] M. Nawaz, A. Heitor, M. Sivakumar, Geopolymers in construction - recent developments, Constr. Build. Mater. 260 (2020) (2020), 120472, https://doi.org/10.1016/j.conbuildmat.2020.120472.
[12] W.D. Callister, D.G. Rethwisch, Materials Science and Engineering: An Introduction, Wiley, New York, 2018.
[13] T. Suwan, M. Fan, Influence of OPC replacement and manufacturing procedures on the properties of self-cured geopolymer, Constr. Build. Mater. 73 (2014) 551–561.
[14] P. Duxson, A, et al., Geopolymer technology: the current state of the art, J. Mater. Sci. 42 (2007) 2917–2933.
[15] T. Suwan, M. Fan, Effect of manufacturing process on the mechanisms and mechanical properties of fly ash-based geopolymer in ambient curing temperature, Mater. Manuf. Process. 32 (5) (2017) 461–467.
[16] S. Adjei, et al., Geopolymer as the future oil-well cement: a review, J. Pet. Sci. Eng. 208 (2022), 109485.
[17] T. Suwan, Development of self-cured geopolymer cement (Doctoral dissertation), Brunel University, London, 2016.
[18] M. Grant Norton, J.L. Provis, 1000 at 1000: Geopolymer technology—the current state of the art, J. Mater. Sci. 55 (28) (2020) 13487–13489.
[19] Y. Wu, et al., Geopolymer, green alkali activated cementitious material: synthesis, applications and challenges, Constr. Build. Mater. 224 (2019) 930–949.
[20] I.G. Lodeiro, et al., Use of industrial by-products as alkaline cement activators, Constr. Build. Mater. 253 (2020), 119000.
[21] C. Panagiotopoulou, et al., Dissolution of aluminosilicate minerals and by-products in alkaline media, J. Mater. Sci. 42 (9) (2007) 2967–2973.
[22] D. Hardjito, C.C. Cheak, C.L. Ing, Strength and setting times of low calcium fly ash-based geopolymer mortar, Mod. Appl. Sci. 2 (4) (2008) 3–11.
[23] D. Hardjito, S.S. Fung, Fly ash-based geopolymer mortar incorporating bottom ash, Mod. Appl. Sci. 4 (1) (2010) 44.
[24] A. Fernández-Jiménez, I. García-Lodeiro, A. Palomo, Durability of alkali-activated fly ash cementitious materials, J. Mater. Sci. 42 (9) (2007) 3055–3065.
[25] D.L. Kong, J.G. Sanjayan, Effect of elevated temperatures on geopolymer paste, mortar and concrete, Cem. Concr. Res. 40 (2) (2010) 334–339.
[26] A. Fernández-Jiménez, A. Palomo, Composition and microstructure of alkali activated fly ash binder: effect of the activator, Cem. Concr. Res. 35 (10) (2005) 1984–1992.
[27] H.M. Khater, Effect of cement kiln dust on geopolymer composition and its resistance to sulfate attack, Green. Mater. 1 (1) (2013) 36–46.
[28] A.M. Rashad, S.R. Zeedan, The effect of activator concentration on the residual strength of alkali-activated fly ash pastes subjected to thermal load, Constr. Build. Mater. 25 (7) (2011) 3098–3107.
[29] H. Zhang, et al., Deterioration of ambient-cured and heat-cured fly ash geopolymer concrete by high temperature exposure and prediction of its residual compressive strength, Constr. Build. Mater. 262 (2020), 120924.
[30] A. Fernández-Jiménez, A. Palomo, Composition and microstructure of alkali activated fly ash binder: effect of the activator, Cem. Concr. Res. 35 (10) (2005) 1984–1992.
[31] A. Mishra, et al., Effect of concentration of alkaline liquid and curing time on strength and water absorption of geopolymer concrete, ARPN J. Eng. Appl. Sci. 3 (1) (2008) 14–18.
[32] F.A. Memon, et al., Effect of sodium hydroxide concentration on fresh properties and compressive strength of self-compacting geopolymer concrete, J. Eng. Sci. Technol. 8 (1) (2013) 44–56.
[33] American Chemistry Council, Inc, 2021. Guide to the Business of Chemistry – 2021: Uses of sodium hydroxide. Retrieved from https://store.americanchemistry.com/products/guide-to-the-business-of-chemistry-2018-electronic-version on May 15th, 2022.
[34] WorldOfChemicals, 2022. Methods of preparation of caustic soda. Retrieved from https://medium.com/@worldofchemical/methods-of-preparation-of-caustic-soda-db79de978236on June 21st, 2022.
[35] Pakalawong, M., 2022. Sodium Hydroxide, DPIM Economic Review, Ministry of Industry. http://www.siamchemi.com/ on June, 21st 2022.
[36] I. Boustead, SODIUM HYDROXIDE, eco-profiles of the european plastics industry, Polym. Convers. Rep. Plast. Eur. Assoc. Plast. Manuf. Rep. (2005) 10.
[37] M. Keawthun, S. Krachodnok, A. Chaisena, Conversion of waste glasses into sodium silicate solutions, Int. J. Chem. Sci. 12 (1) (2014) 83–91.
[38] P. Chindaprasirt, T. Chareerat, S. Hatanaka, T. Cao, High-strength geopolymer using fine high-calcium fly ash, J. Mater. Civ. Eng. 23 (3) (2011) 264–270.

[39] S.A. Roberts, R.E. Cameron, The effects of concentration and sodium hydroxide on the rheological properties of potato starch gelatinisation, Carbohydr. Polym. 50 (2) (2002) 133–143.
[40] Pujiastuti, C., Ngatilah, Y., Sumada, K. and Muljani, S., 2018. The effectiveness of sodium hydroxide (NaOH) and sodium carbonate (Na2CO3) on the impurities removal of saturated salt solution. In Journal of Physics: Conference Series (Vol. 953, No. 1, p. 012215). IOP Publishing.
[41] Pakalawong, M. (2018). Sodium Hydroxide, DPIM Economic Review, Ministry of Industry. Retrieved from http://www.siamchemi.com/. On 30 July 2019.
[42] Boustead, I. (2005). SODIUM HYDROXIDE. Eco-profiles of the European Plastics Industry. Report for Plastics Europe Association of plastic manufacturer.
[43] B. Traynor, H. Uvegi, E. Olivetti, B. Lothenbach, R.J. Myers, Methodology for pH measurement in high alkali cementitious systems, Cem. Concr. Res. 135 (2020), 106122.
[44] T. Suwan, M. Fan, N. Braimah, Micro-mechanisms and compressive strength of Geopolymer-Portland cementitious system under various curing temperatures, Mater. Chem. Phys. 180 (2016) 219–225.
[45] R. Çetintaş, S. Soyer-Uzun, Relations between structural characteristics and compressive strength in volcanic ash based one–part geopolymer systems, J. Build. Eng. 20 (2018) 130–136.
[46] Adelizar, A.S., et al., 2020. Fly ash and bottom ash utilization as geopolymer: Correlation on compressive strength and degree of polymerization observed using FTIR. *IOP Conference Series: Materials Science and Engineering*, 742(1), p. 012042.
[47] C. Bertagnolli, M.G.C.D. Silva, Characterization of Brazilian Bentonite Organoclays as sorbents of petroleum-derived fuels, Mater. Res. 15 (2) (2012), 253259.
[48] S. Gomes, M. François, Characterization of mullite in silicoaluminous fly ash by XRD, TEM, and 29Si MAS NMR, Cem. Concr. Res. 30 (2) (2000) 175–181.
[49] A. Nikvar-Hassani, L. Manjarrez, L. Zhang, Rheology, setting time, and compressive strength of class F Fly ash–based geopolymer binder containing ordinary portland cement, J. Mater. Civ. Eng. 34 (1) (2022), 04021375.
[50] T. Suwan, M. Fan, N. Braimah, Internal heat liberation and strength development of self-cured geopolymers in ambient curing conditions, Constr. Build. Mater. 114 (2016) 297–306.
[51] T. Suwan, et al., Properties and microstructures of crushed rock based-alkaline activated material for roadway applications, Materials 15 (9) (2022) 3181.